

Quasi-classical dynamics of interacting Bose condensates[†]

A. N. Salgueiro⁽¹⁾, M. C. Nemes⁽²⁾,
M. D. Sampaio⁽²⁾ and A. F. R. de Toledo Piza⁽¹⁾.

⁽¹⁾*Instituto de Física, Universidade de São Paulo
CP 20516, 01452-990 São Paulo, S.P., Brazil*

⁽²⁾*Departamento de Física, ICEX, Universidade Federal de Minas Gerais
C.P. 702, 30161-970 Belo Horizonte, M.G., Brazil*

Abstract

The dynamics of the composition of uniform Bose condensates involving two species capable of reciprocal interconversion is treated in terms of a collective quasi-spin model. This collective model quickly reduces to classical form towards the thermodynamic limit. Quantum solutions are easily obtained numerically short of this limit which give insight into the dynamically relevant correlation processes.

September 1, 1998

PACS numbers: 03.75.Fi, 05.30.Jp, 03.65.Sq, 42.50.Fx

[†]Supported in part by Fundação de Amparo à Pesquisa do Estado de São Paulo (FAPESP) and Conselho Nacional de Desenvolvimento Científico e Tecnológico (CNPq), Brazil.

1 Introduction

After dilute condensates of bosonic atoms were produced and observed in the laboratory by Cornell [1], considerable interest arose concerning the dynamics of the more complex system formed by two coexisting, coupled condensates [2, 3]. In ref. [3] the dynamics of component separation of a magnetically trapped dual condensate has been studied by making use of the possibility of adjusting independently the trapping conditions for each of the two components. In this case the composition of the mixture remains fixed, and the finite size of the system plays an essential role. Other situations, in which the coupling allows for interconversion between the two condensate types, have also been considered from a theoretical point of view. Here, even under equilibrium conditions for which the spatial dynamics of the trapped condensate particles is essentially frozen, one still has to consider the interesting collective dynamics of the composition of the dual condensate. One of the situations that has been considered in this connection involves two different internal states of the atoms, as in refs. [2, 3]. In this case, the interconversion coupling is provided by laser-induced Raman transitions between these two states [4]. More recently, the observation of effects of the so called Feshbach resonances in atomic Bose condensates [5] led to the consideration of possible experimental situations involving coupled atomic and molecular condensates, the latter occurring in the two-atom channel responsible for the resonance phenomenon [6, 7]. In this paper we explore the fact that, by making use of the assumption of frozen spatial dynamics, the dynamics of condensate composition can in both cases be treated in terms of simple collective variables which evolve in an essentially classical regime, quantum numbers being of the order of the number of atoms involved in the condensate. We can thus derive classical, canonical equations of motion governing the model composition dynamics.

2 Effective dynamics of coupled condensates

Although from a microscopic point of view the dual trapped condensate dynamics involves many quite subtle questions of atomic physics, once these are duly tamed to the point where they can be manipulated in the laboratory it is possible to encapsulate their effect in a few dynamical parameters for the purpose of studying the overall behavior of the condensate. Theoretically, the two above mentioned cases have thus been modeled in terms of an effective Hamiltonian density of the form [4, 6, 7]

$$\mathcal{H} = \mathcal{H}_a + \mathcal{H}_b + \mathcal{H}_c \tag{1}$$

where the first two terms describe the individual condensates, i.e.

$$\mathcal{H}_{a,b} = \phi_{a,b}^* \left[-\frac{\hbar^2 \nabla^2}{2m_{a,b}} + \epsilon_{a,b} + \frac{\lambda_{a,b}}{2} |\phi_{a,b}|^2 \right] \phi_{a,b} \tag{2}$$

and the last term contains the coupling of the two condensates. For the atom-atom (*AA*) case it is written as

$$\mathcal{H}_c^{(AA)} = \lambda |\phi_a|^2 |\phi_b|^2 + \alpha(\phi_a^* \phi_b + \phi_b^* \phi_a) \quad (3)$$

while for the atom-molecule (Feshbach resonance, *FR*) case it reads

$$\mathcal{H}_c^{(FR)} = \lambda |\phi_a|^2 |\phi_b|^2 + \alpha(\phi_a^{*2} \phi_b + \phi_b^* \phi_a^2). \quad (4)$$

The parameters $\epsilon_{a,b}$ represent possibly different intrinsic energies in the two boson channels. Their elastic interaction is described in terms of pseudopotential parameters $\lambda_{a,b}$, λ and channel coupling is represented by the parameter α . In the *AA* case considered by Zoller [4] the latter involves the intensity of the laser responsible for the Raman transitions, and should therefore be considered as an externally determined control parameter. In the *FR* case, on the other hand, α stands for the coupling to the quasi-bound molecular state responsible for the resonance and therefore determining its width, while $\epsilon_b - 2\epsilon_a$ represents the “detuning” away from the resonance, controlled externally by means of an applied magnetic field [5].

For sufficiently extended and uniform systems the effective field operators ϕ_a , ϕ_b can be usefully expanded in a momentum basis as

$$\phi_a(\vec{r}) = \frac{1}{\sqrt{V}} \sum_{\vec{k}} e^{i\vec{k}\cdot\vec{r}} a_{\vec{k}}, \quad \phi_b(\vec{r}) = \frac{1}{\sqrt{V}} \sum_{\vec{k}} e^{i\vec{k}\cdot\vec{r}} b_{\vec{k}},$$

where the nonhermitean mode operators $a_{\vec{k}}$, $b_{\vec{k}}$ satisfy standard bosonic commutation relations. Furthermore, the depletion due to correlations being small in low density systems [8], in the condensate regime essentially all the bosons are in the zero momentum mode, so that the relevant Hamiltonian density reduces to the simple single-mode form (for simplicity we omit the zero momentum label in this case)

$$\mathcal{H}_a \rightarrow \frac{\epsilon_a}{V} a^\dagger a + \frac{\lambda_a}{2V^2} a^\dagger a^\dagger a a,$$

a similar expression for \mathcal{H}_b and

$$\mathcal{H}_c^{(AA)} \rightarrow \frac{\lambda}{V^2} a^\dagger b^\dagger b a + \frac{\alpha}{V} (a^\dagger b + b^\dagger a), \quad (5)$$

$$\mathcal{H}_c^{(FR)} \rightarrow \frac{\lambda}{V^2} a^\dagger b^\dagger b a + \frac{\alpha}{V^{3/2}} (a^\dagger a^\dagger b + b^\dagger a a) \quad (6)$$

for the atom-atom and Feshbach resonance cases respectively. In both cases the total number of atoms (namely, $a^\dagger a + b^\dagger b$ in the *AA* case and $a^\dagger a + 2b^\dagger b$ in the *FR* case) is obviously conserved. Exact single mode coupled condensate solutions can therefore be obtained through the diagonalization of finite matrices. Furthermore, the single mode coupled condensate Hamiltonians belong to the special class of the so called Curie-Weiss models [9], for which

the mean-field approximation becomes exact in the thermodynamic limit (number of particles $\rightarrow \infty$ at constant density). In order to explore this latter feature, it is convenient to express $\mathcal{H}^{(AA)}$ and $\mathcal{H}^{(FR)}$ in terms of alternate dynamic variables, which can be conveniently chosen so as to obey standard SU(2) commutation relations.

2.1 Two atomic condensates

In the AA case, the appropriate variables are just the well known Schwinger realization of the SU(2) algebra in terms of two types of bosons [10]

$$J_z = \frac{1}{2}(a^\dagger a - b^\dagger b); \quad J_+ = J_-^\dagger = a^\dagger b.$$

In this case the Casimir operator \vec{J}^2 appears as $J(J+1)$ with $J = \frac{1}{2}(a^\dagger a + b^\dagger b)$, half the number of atoms, and the Hamiltonian density can be written as

$$\begin{aligned} \mathcal{H}^{(AA)} = & \frac{\epsilon_a + \epsilon_b}{V} J + \frac{\epsilon_a - \epsilon_b}{V} J_z + \frac{\lambda_a}{2V^2} (J + J_z)(J + J_z - 1) + \frac{\lambda_b}{2V^2} (J - J_z)(J - J_z - 1) \\ & + \frac{\lambda}{V^2} (J^2 - J_z^2) + \frac{\alpha}{V} (J_+ + J_-). \end{aligned}$$

In order to take the thermodynamic limit it is more convenient to work with the scaled Hamiltonian $h^{(AA)} \equiv V\mathcal{H}^{(AA)}/J$ which reads

$$\begin{aligned} h^{(AA)} = & \epsilon_a + \epsilon_b + (\epsilon_a - \epsilon_b) \frac{J_z}{J} + \frac{n\lambda_a}{4} \left(1 + \frac{J_z}{J}\right) \left(1 + \frac{J_z}{J} - \frac{1}{J}\right) \\ & + \frac{n\lambda_b}{4} \left(1 - \frac{J_z}{J}\right) \left(1 - \frac{J_z}{J} - \frac{1}{J}\right) + \frac{n\lambda}{2} \left(1 - \frac{J_z^2}{J^2}\right) + 2\alpha \frac{J_x}{J} \end{aligned} \quad (7)$$

where the atom density $n = 2J/V$ has been introduced. The thermodynamic limit consists now in letting $J \rightarrow \infty$ at constant n . The spectrum of the scaled components J_i/J remains bounded in the closed interval $[-1, +1]$ and becomes increasingly dense as J is increased. The thermodynamic limit corresponds therefore to the classical limit of a dimensionless angular momentum-like algebra which may be formally characterized as

$$\lim_{J \rightarrow \infty} \frac{J}{i} \left[\frac{J_k}{J}, \frac{J_l}{J} \right] \equiv \{j_k, j_l\} = \epsilon_{klm} j_m \equiv \epsilon_{klm} \lim_{J \rightarrow \infty} \frac{J_m}{J} \quad (8)$$

where the curly brackets now denote a Poisson bracket. In the thermodynamic limit, Eq. (7) yields the (quasi-)classical expression for the scaled energy

$$\begin{aligned}
h_{qc}^{(AA)} &= \epsilon_a + \epsilon_b + (\epsilon_a - \epsilon_b)j_z + \frac{n\lambda_a}{4}(1 + j_z)^2 + \frac{n\lambda_b}{4}(1 - j_z)^2 \\
&\quad + \frac{n\lambda}{2}(1 - j_z^2) + 2\alpha j_x.
\end{aligned} \tag{9}$$

Alternatively, one can express Eq. (9) as a proper Hamiltonian function, in terms of a pair of canonically conjugate variables. One such pair which is quite convenient has been previously obtained using the quantum kinematical scheme developed by Schwinger in terms of unitary operator bases [11] and the associate (discrete) Weyl-Wigner transforms [12]. After carrying out the thermodynamic limit in the way just described, one finds that the (angle) variable which is canonically conjugate to the (“action”) variable j_z is just the azimuthal angle φ , so that j_x can be expressed canonically as

$$j_x = \sqrt{1 - j_z^2} \cos \varphi. \tag{10}$$

Using this fact, one may derive from Eq. (9) equations of motion for the variables j_z and φ . A technical point to be observed here is that the dimensionless character of the “action” variable j_z corresponds to measuring time in inverse energy units. In order to introduce an appropriate time scale one may write, consistently with Eq. (8),

$$\frac{dj_z}{dt} = \lim_{J \rightarrow \infty} \frac{d}{dt} \frac{J_z}{J} = \lim_{J \rightarrow \infty} \frac{J}{i\hbar} \left[\frac{J_z}{J}, \frac{V\mathcal{H}^{(AA)}}{J} \right] \equiv \left\{ j_z, \frac{h_{qc}^{(AA)}}{\hbar} \right\} \tag{11}$$

which gives

$$\frac{d\varphi}{dt} = \frac{\partial h_{qc}^{(AA)}}{\hbar \partial j_z} = \frac{\epsilon_a - \epsilon_b}{\hbar} + \frac{n\lambda_a}{2\hbar}(1 + j_z) - \frac{n\lambda_b}{2\hbar}(1 - j_z) - \frac{n\lambda}{\hbar} j_z - \frac{2\alpha j_z}{\hbar \sqrt{1 - j_z^2}} \cos \varphi \tag{12}$$

$$\frac{dj_z}{dt} = -\frac{\partial h_{qc}^{(AA)}}{\hbar \partial \varphi} = \frac{2\alpha}{\hbar} \sqrt{1 - j_z^2} \sin \varphi.$$

In order to explore further the significance of the canonical variable φ it is useful to derive the second Eq. (12) in the following alternate way. The (zero momentum) field operators ϕ_a and ϕ_b satisfy the coupled nonlinear equations

$$\begin{aligned}
i\hbar \dot{\phi}_a &= (\epsilon_a + \lambda_a |\phi_a|^2 + \lambda |\phi_b|^2) \phi_a + \alpha \phi_b \\
i\hbar \dot{\phi}_b &= (\epsilon_b + \lambda_b |\phi_b|^2 + \lambda |\phi_a|^2) \phi_b + \alpha \phi_a.
\end{aligned}$$

From these one may easily derive the equations for $|\phi_a|^2$ and $|\phi_b|^2$

$$i\hbar \frac{d}{dt} |\phi_a|^2 = 2i\alpha \operatorname{Im} \phi_b \phi_a^* \quad (13)$$

$$i\hbar \frac{d}{dt} |\phi_b|^2 = -2i\alpha \operatorname{Im} \phi_b \phi_a^*$$

which show an explicit dependence on the phase of $\phi_b \phi_a^*$. Writing this object as $|\phi_b| |\phi_a| e^{i\delta^{(AA)}}$ the difference of these equations appears as

$$\hbar \frac{d}{dt} (|\phi_a|^2 - |\phi_b|^2) = 4\alpha |\phi_b| |\phi_a| \sin \delta^{(AA)}$$

while their sum merely gives the conservation of the total number of atoms. Using the definitions of J and J_z one has

$$|\phi_a|^2 - |\phi_b|^2 \equiv \frac{2J_z}{J}; \quad |\phi_b| |\phi_a| \equiv \frac{1}{V} \sqrt{(J + J_z)(J - J_z)}$$

so that the difference equation becomes

$$\frac{d}{dt} \frac{J_z}{J} = \frac{2\alpha}{\hbar} \sqrt{1 - \frac{J_z^2}{J^2}} \sin \delta^{(AA)}.$$

This corresponds to the second Eq. (12) and furthermore identifies the angle variable φ with the phase $\delta^{(AA)}$.

The density dependence of the Hamiltonian Eq. (9) also gives a direct analytical expression for the pressure exerted by the interacting condensates. One has in fact

$$P^{(AA)} \equiv n^2 \frac{\partial h_{qc}^{(AA)}}{\partial n} = \frac{n^2}{4} \left[\lambda_a (1 + j_z)^2 + \lambda_b (1 - j_z)^2 + 2\lambda (1 - j_z^2) \right] \quad (14)$$

In order to avoid the collapse of stationary states this expression must be positive when evaluated at the equilibrium value of j_z .

2.2 Feshbach-resonant atomic-molecular condensates

The *FR* case, on the other hand, can be treated in precisely the same way once an appropriate realization of the $SU(2)$ algebra is constructed. To this effect, consider the case in which there are N atoms present. The relevant finite dimensional space in which $\mathcal{H}^{(FR)}$ is to be diagonalized is then generated by base vectors of the form $|N - 2n_b, n_b\rangle$, where the two labels denote the number of atoms and the number of molecules respectively. For definiteness, N will be assumed to be even, so that n_b runs from zero to $N/2$. The next step is to identify this basis with the J_z eigenstates of a $SU(2)$ multiplet associated with the eigenvalue $N/4(N/4+1)$

of the Casimir operator. A convenient way of doing so is to identify the eigenvalue of J_z with $n_b - N/4$, so that $J_z = \frac{1}{4}(2b^\dagger b - a^\dagger a)$ and

$$|N - 2n_b, n_b\rangle \leftrightarrow |J = \frac{N}{4}, J_z = n_b - \frac{N}{4}\rangle.$$

If one then defines J_\pm in terms of their standard action on the J_z eigenstates, i.e.

$$J_\pm |J, J_z\rangle = \sqrt{J(J+1) - J_z(J_z \pm 1)} |J, J_z \pm 1\rangle$$

one finds, after a straightforward calculation,

$$J_+ = \frac{1}{\sqrt{2(a^\dagger a + 1)}} a a b^\dagger; \quad J_- = a^\dagger a^\dagger b \frac{1}{\sqrt{2(a^\dagger a + 1)}}.$$

The FR Hamiltonian density can now be written in the form

$$\begin{aligned} \mathcal{H}^{(FR)} = & \frac{\epsilon_b + 2\epsilon_a}{V} J + \frac{\epsilon_b - 2\epsilon_a}{V} J_z + \frac{\lambda_a}{V^2} 2(J - J_z)(J - J_z - 1) + \frac{\lambda_b}{2V^2} (J + J_z)(J + J_z - 1) \\ & + \frac{\lambda}{V^2} 2(J^2 - J_z^2) + \frac{\alpha}{V^{3/2}} \left(J_- \sqrt{4(J - J_z) + 2} + \sqrt{4(J - J_z) + 2} J_+ \right) \end{aligned}$$

and the corresponding J -scaled Hamiltonian, after taking the thermodynamic limit, becomes

$$\begin{aligned} h_{qc}^{(FR)} & \equiv \lim_{J \rightarrow \infty} \frac{V \mathcal{H}^{(FR)}}{J} \\ & = \epsilon_b + 2\epsilon_a + (\epsilon_b - 2\epsilon_a) j_z + \frac{n\lambda_a}{2} (1 - j_z)^2 + \frac{n\lambda_b}{8} (1 + j_z)^2 + \frac{n\lambda}{2} (1 - j_z^2) \\ & \quad + 2\alpha \sqrt{n} \sqrt{1 - j_z} j_x \end{aligned} \tag{15}$$

where the vanishing of the commutators $[\frac{J_z}{J}, \frac{J_\pm}{J}]$ in this limit has been used to obtain the last term. An interesting feature of these Hamiltonians is the quenching of the coupling term involving α when the molecular component is dominant (J_z close to J or j_z close to 1). It can be traced ultimately to the feature of Bose statistics which associates the factor $\sqrt{(N - 2n_b + 1)(N - 2n_b + 2)n_b}$ to the amplitude for converting one molecule into two atoms when there are n_b molecules present. This factor in fact decreases faster than that associated with the plain J_- operator when n_b is large (close to its maximum value $N/2$).

One may next adopt again the canonical form of j_x given in Eq. (10) and the appropriate time scale to write the equations of motion

$$\begin{aligned} \frac{d\varphi}{dt} & = \frac{\epsilon_b - 2\epsilon_a}{\hbar} - \frac{n\lambda_a}{\hbar} (1 - j_z) + \frac{n\lambda_b}{4\hbar} (1 + j_z) - \frac{n\lambda}{\hbar} j_z - \frac{\alpha\sqrt{n}}{\hbar} \frac{1 + 3j_z}{\sqrt{1 + j_z}} \cos \varphi \\ \frac{dj_z}{dt} & = \frac{2\alpha\sqrt{n}}{\hbar} (1 - j_z) \sqrt{1 + j_z} \sin \varphi. \end{aligned} \tag{16}$$

In a way which is completely analogous to the *AA* case one may here identify the canonical variable φ with the phase $\delta^{(FR)}$ defined as

$$\phi_a^2 \phi_b^* \equiv |\phi_a|^2 |\phi_b| e^{i\delta^{(FR)}}.$$

The pressure can also be obtained in this case with the result

$$P^{(FR)} = \frac{n^2}{2} \left[\lambda_a (1 - j_z)^2 + \frac{\lambda_b}{4} (1 + j_z)^2 + \lambda (1 - j_z^2) \right] + \alpha n^{3/2} (1 - j_z) \sqrt{1 + j_z} \cos \varphi, \quad (17)$$

which reproduces (with different notation) the result obtained in ref. [6]. When the square brackets are positive for the equilibrium value of j_z , one may still have a domain of negative pressures at low densities when the coefficient of $n^{3/2}$ is negative. Also as observed in [6], this implies that the system becomes “self-bound” and saturates at the value of n for which the pressure vanishes.

In order to make the model sufficiently realistic for the *FR* system it is important to take into account the loss of atoms which may be expected due to an enhanced rate of inelastic collisions involving the molecular channel directly [5, 7]. This loss has in fact been used as a signal to detect the Feshbach resonance in ref. [5]. The simplest way of including the loss of atoms consists in adding appropriate master loss-terms to the equations of motion for the atomic and molecular densities, n_a and n_b . Under loss-free conditions, we may use the expressions

$$n_a = \frac{1 - j_z}{2} n, \quad n_b = \frac{1 + j_z}{4} n \quad (18)$$

and the equation of motion for j_z , Eq. (16), to write

$$\begin{aligned} \frac{dn_a}{dt} &= -\frac{n}{2} \frac{dj_z}{dt} = -\frac{\alpha n^{3/2}}{\hbar} (1 - j_z) \sqrt{1 + j_z} \sin \varphi \\ \frac{dn_b}{dt} &= \frac{n}{4} \frac{dj_z}{dt} = \frac{\alpha n^{3/2}}{2\hbar} (1 - j_z) \sqrt{1 + j_z} \sin \varphi. \end{aligned}$$

These equations are the *FR* analogs of Eqs. (13), used to identify the canonical variable φ with the phase of an appropriate combination of field variables. To take loss effects into account these equations are replaced by

$$\begin{aligned} \frac{dn_a}{dt} &= -\frac{\alpha n^{3/2}}{\hbar} (1 - j_z) \sqrt{1 + j_z} \sin \varphi - c_{aa} n_a^2 - c_{ab} n_b n_a \\ \frac{dn_b}{dt} &= \frac{\alpha n^{3/2}}{2\hbar} (1 - j_z) \sqrt{1 + j_z} \sin \varphi - c_{bb} n_b^2 - c_{ba} n_a n_b \end{aligned}$$

which involve four loss-rate coefficients c_{ij} . These are defined so that $c_{ij}n_j$ represents the decay constant of the i -boson density due to collisions with j -bosons. The important decay rates in the molecular channel thus imply larger values of c_{bb} and c_{ba} when compared with c_{aa} and c_{ab} . The time evolution of the total density n is now determined by the equation

$$\frac{dn}{dt} = 2\frac{dn_b}{dt} + \frac{dn_a}{dt} = -\frac{n^2}{8} \left[2c_{aa}(1-j_z)^2 + c_{bb}(1+j_z)^2 + (c_{ab} + c_{ba})(1-j_z^2) \right] \quad (19)$$

which must be solved together with Eqs. (16) in order to include atomic losses in the dynamics of the interacting condensates. It should be noted that this procedure corresponds exactly to that adopted in ref. [7], where one works with the nonlinear equations of motion for the fields ϕ_a, ϕ_b modified to have complex pseudopotential parameters. In fact, the terms involving the imaginary parts of these parameters cancel from the equation of motion for the variable j_z , but give non vanishing contributions to dn/dt which exactly reproduce Eq. (19).

3 Numerical results

In order to explore the classical propensities of the quantum, Curie-Weiss coupled condensate dynamics, it is most convenient to make use of a phase-space quantum description. An appropriate description of this sort, for systems evolving in quantum phase spaces of finite dimensionality, consists of the discrete action-angle Weyl-Wigner representation used in Ref. [12]. In the next few lines we simply collect the final prescription to obtain the discrete transforms, and refer the interested reader to this reference for further details. For a state $|a\rangle$ represented in the appropriate multiplet base $|J, m\rangle$ as

$$|a\rangle = \sum_{m=-J}^J a_m |J, m\rangle$$

one first constructs the matrix

$$r(k, l) = \frac{1}{\sqrt{2J+1}} \sum_{m=-J}^J a_m a_{\{m+l\}}^* \exp \left[-\frac{2\pi i}{2J+1} k \left(m + \frac{l}{2} \right) \right]$$

where the range of the integers k and l is $-J \leq k, l \leq J$ and the index $\{m+l\}$ denotes the value of $m+l$ cyclically confined to the range $-J, J$ of the basis labels. Explicitly, one has

$$\{m+l\} = m+l - (2J+1) \text{ Floor} \left(\frac{m+l+J}{2J+1} \right)$$

where $\text{Floor}(x)$ denotes the *larger* integer (negative for $x < 0$) less than or equal to x . The desired discrete Wigner phase-space representative $a_w(p, q)$ of the state $|a\rangle$ is then obtained as the double (discrete) Fourier transform

$$(2J + 1) a_w(p, q) = \frac{1}{\sqrt{2J + 1}} \sum_{k,l} \exp \left[\frac{2\pi i}{2J + 1} (pk + ql) \right] r(k, l).$$

In this expression the range of the integers p and q is also bounded as $-J \leq p, q \leq J$, and the properly scaled variables corresponding to j_z and φ are q/J and $2\pi p/(2J + 1)$ respectively. The Weyl transform of the Hamiltonian can be obtained in exactly the same way, replacing the amplitude products $a_m a_{\{m+l\}}^*$ by the matrix elements $\langle J, m | V\mathcal{H}/J | J, \{m + l\} \rangle$ multiplied by the number of states $2J + 1$, when evaluating $r(k, l)$.

3.1 Two atomic condensates

We restrict our numerical treatment of the composition dynamics of two atomic condensates to the “symmetric” case, in the sense of ref. [4], i.e. $\epsilon_a = \epsilon_b \equiv 0$ (implying a suitable definition of the energy scale) and $\lambda_a = \lambda_b \equiv \lambda_0$. Furthermore, we adopt units such that the atom density $n = 1$ and $\hbar = \lambda_0 = 1$ so that energies are given in units of $\lambda_0 n$, times are given in units of $\hbar/\lambda_0 n$ and the various possible situations will unfold by varying the remaining parameters, λ , α and, when short of the thermodynamic limit, $J \equiv N/2$, cf. Eqs. (7) and (9).

The numerical spectrum of $h^{(AA)}$, Eq. (7), is given for $\lambda = 1.5$, $\alpha = .1$ and $J = 20$ in Fig. 1, together with the mean b -type atom numbers $\langle n_b \rangle \equiv \langle b^\dagger b \rangle$ and variances $\sigma_b \equiv \sqrt{\langle (b^\dagger b)^2 \rangle - \langle n_b \rangle^2}$ for each of the corresponding eigenstates. The states with energy $E_k < 1$ are in fact nearly degenerate doublets (see Fig. 5 below) of “Schrödinger cat states”, consisting of superpositions of basis states with $\langle n_b \rangle \sim 0$ and $\langle n_b \rangle \sim N$ [4]. The large values of σ_b for these states signal the large, strongly correlated fluctuations of n_b and n_a . The doublet structure can be immediately understood with reference to the Weyl transform of $h^{(AA)}$, shown in Fig. 2 together with the quasi-classical energy surface corresponding to $h_{qc}^{(AA)}$: it results from the symmetric minima near $j_z = \pm 1$ separated by the barrier which peaks at $j_z = 0$. As also discussed in ref. [4], this situation results from having $\lambda > \lambda_0$ and small enough α (“weak laser” case). The energy splitting of the doublet members approaches zero as J is increased, leading to degeneracy in the thermodynamic limit. The Wigner functions corresponding to each state in the lowest doublet for $J = 20$ are shown in Fig. 3. The lowest (highest) member of the doublet involves a symmetric (anti-symmetric) superposition of states $|J, M\rangle$ strongly concentrated on the largest values of $|M|$. The Wigner functions show moreover that these states are strongly peaked also in the conjugate angle variable, as a result of the dips of the energy surface at $\varphi = \pm\pi$. Increasing α will depress the pass along the $\varphi = \pi$ line leading eventually to a minimum at $j_z = 0$ and therefore to ground states dominated by small $|M|$ components. This is shown in Fig. 4, where the probabilities $p(M) \equiv |\langle J, M | \text{g.s.} \rangle|^2$ are plotted against M for a range of values of α .

A most dramatic consequence of the strong collective character of the composition dynamics as described by the Hamiltonian $h^{(AA)}$, Eq. (7), is that, as was pointed out before

(see e.g. ref. [13]), a suitably scaled distribution of the energy eigenvalues quickly approaches the quasi-classical distribution in which the fraction of levels with eigenvalue smaller than a given energy is proportional to the area of the phase-space domain in which the quasi-classical energy is less than this value. This ultimately allows associating energy eigenstates with phase-space trajectories on an essentially one to one basis. Fig. 5 illustrates this feature showing the fraction of the total number of states having energy less than E as a function of E for several values of J together with the quasi-classical limit. One sees there that even the case $N=20$ is already fairly close to the quasi-classical limit from which it differs mainly by an overall translation in energy related to the terms of order $1/J$ in Eq. (7). Also visible is the staggering associated with the doublet structure of the $\lambda > \lambda_0$, “weak laser” case, which persists up to energies close to that corresponding to the separatrix going through the highest point of the $\varphi = \pi$ pass at $j_z = 0$ ($E = 1.05$ for this example, in the quasi-classical limit). An enhancement of the level density at this energy is also clearly visible.

3.2 Feshbach-resonant atomic-molecular condensates

While in the AA case the relevant external control parameter is the intercondensate coupling α , associated with laser intensity, in the case of realistic FR systems the relevant parameter is the detuning $\delta \equiv \epsilon_a - 2\epsilon_b$, controlled by an externally applied uniform magnetic field. In order to illustrate the composition dynamics in this case we take $\lambda_a = \lambda_b = \lambda = 1$ and again choose units such that $\hbar = n = 1$, the zero of the energy scale being defined so that $\epsilon_a = 0$. The remaining parameters to be considered are therefore α , here related to the resonance width, the detuning parameter ϵ_b , which is the intrinsic energy difference between one molecule and two atoms, and (again when short of the thermodynamic limit) $J \equiv N/4$.

The numerical quantum spectrum of $V\mathcal{H}^{(FR)}/J$ is given in Fig. 6 (similar to Fig. 1, corresponding to the AA case) for $\alpha = \sqrt{2}/2$, $\epsilon_b = 2$ and $J = 20$. The mean molecule number $\langle n_b \rangle$ and variance σ_b for the eigenstates are shown at the corresponding energy eigenvalues. The Weyl transform of the quantum Hamiltonian is shown in Fig. 7, together with its classical limit, Eq. (15). The scaling property of the level density with J , analogous to that shown in Fig. 5 for the AA case, is shown in Fig. 8.

In this case, the quantum ground state is strongly localized, both in action and angle variables, in the non-degenerate minimum of the energy surface, as shown by its Wigner function, Fig. 9. Increasing the value of the detuning parameter energetically favors the lower M components in the ground state, which becomes eventually an essentially pure atomic condensate, as can be seen in Fig. 10, where $\epsilon_b = 50$ with no change in the remaining parameters. This figure shows the Weyl energy surface for this case and also the Wigner function of the corresponding ground state. Since this energy surface is dominated by the detuning term, and therefore rendered only very weakly dependent on the angle variable, its ground state appears as strongly delocalized in this variable for $J = 20$. The definition of this ground state in the angle variable is however expected to increase for larger values of J , as a more collective state fits in the very shallow minimum which persists at $\varphi = \pi$, near

$j_z = -1$.

Next we use the $\epsilon_b = 50$ quantum ground state as an initial condition in order to obtain numerically the (loss free) quantum evolution under the $\epsilon_b = 2$ Hamiltonian. This corresponds to the scheme devised in ref. [7], in which the ground state is prepared at some initial large value of the detuning which, is then suddenly reduced by adjusting the applied external magnetic field. The absolute square coefficients of the decomposition of the initial state in the $\epsilon = 2$ eigenstates are shown in Fig. 11, and the resulting time dependence of the mean value of J_z/J for $J = 20$ are shown in Fig. 12 together with the corresponding time-dependent variances. The mean number of atoms and of molecules, $\langle n_a \rangle$ and $\langle n_b \rangle$, are related to $\langle J_z \rangle/J$ simply as

$$\langle n_a \rangle = 2J \left[1 - \frac{\langle J_z \rangle}{J} \right], \quad \langle n_b \rangle = J \left[1 + \frac{\langle J_z \rangle}{J} \right]$$

and will therefore oscillate with opposite phases as a result of the conservation of the total number of atoms in this calculation. Also shown in the same plot is the function $j_z(t)$ obtained by integrating numerically Eqs. (16) with $\epsilon_b = 2$, $\alpha = \sqrt{2}/2$ and using the phase-space coordinates of the quasi-classical equilibrium point corresponding to $\delta = 50$ as initial conditions. Note that, in view of Eq. (11), the appropriate time parameter to be used in the quantum calculation in order to compare with the quasi-classical result corresponds to solving the Heisenberg equation of motion

$$\frac{i\hbar}{J} \frac{d}{dt} \left[\frac{J_z}{J} \right] = \left[\frac{J_z}{J}, \frac{V\mathcal{H}(FR)}{J} \right]$$

with $J = 20$ in this case. The similarity of the two graphs illustrates the relevance of the quasi-classical calculation of collective properties of the system already for $J = 20$.

Finally, we include the phenomenological loss terms in the quasi-classical equations of motion by integrating simultaneously Eqs. (16) and Eq. (19) with the realistic values of the loss-rate coefficients used in ref. [7], namely $c_{aa} = c_{ab} = 0$ and $c_{bb} = c_{ba} = 0.5$, in the units adopted here. Fig. 13 shows the resulting time evolution of $j_z(t)$ and of $n(t)$, the latter quantity being measured in units of the initial density $n(t=0) = 1$. The atomic and molecular densities are now given by Eq. (18). Their decrease is due mainly to the decrease of the total density n since, as can be seen in Fig. 13, the amplitude of the oscillations of j_z remains relatively immune to the loss effects. Furthermore, the undulating behavior in the decrease of $n(t)$ reflects the asymmetry of the adopted values of the loss-rate coefficients, as a result of which the losses take place in the molecular channel only. This in fact causes the effective loss rate of $n(t)$ to vanish as $j_z(t)$ approaches its lower bound.

4 Concluding comments

The fact that the composition dynamics of essentially undepleted, coupled uniform Bose condensates can be completely reduced to a very compact form in terms of collective variables

only is a direct consequence of the Curie-Weiss character of the underlying model Hamiltonians. While the terms included in these Hamiltonians have been restricted here to those considered earlier [4, 6], the inclusion of other terms, such as two molecule collisions leading to four condensate atoms and atom-molecule collisions leading to three condensate atoms in the Feshbach resonance case, is completely straightforward as they can be readily expressed also in terms of the same collective variables. Not only the resulting collective Hamiltonians reduce to classical form in the thermodynamic limit, but it is also an easy matter to obtain complete numerical quantum solutions short enough of this limit. The study of these solutions indicates that the quasi-classical thermodynamic limit is approached rather fast, while allowing for insight into the dynamically relevant correlation processes.

It should be kept in mind, however, that purely collective dynamical treatments of this kind involve a severe truncation of the full model problem as stated e.g. in Eqs. (1) to (4). In particular, collective excitations will in general couple to depletion effects which fall beyond a purely collective description. We believe nevertheless that the remarkable simplicity of the latter readily provides useful information on such systems and may give useful indications for the development of more complete treatments.

References

- [1] M. H. Anderson, J. R. Ensher, M. R. Matthews, C. E. Wieman and E. A. Cornell, *Science* **269**, 198 (1995).
- [2] C. J. Myatt, E. A. Burt, R. W. Ghrist, E. A. Cornell and C. E. Wieman, *Phys. Rev. Lett.* **78**, 586 (1997).
- [3] D. S. Hall, M. R. Matthews, J. R. Ensher, C. E. Wieman and E. A. Cornell, e-print cond-mat/9804138.
- [4] J. I. Cirac, M. Lewenstein, K. Mølmer and P. Zoller, *Phys. Rev.* **A57**, 1208 (1998).
- [5] S. Inouye, M. R. Andrews, J. Stenger, H.-J. Miesner, D. M. Stamper-Kurn and W. Ketterle, *Nature* **392**, 151 (1998).
- [6] P. Tommasini, E. Timmermans, M. S. Hussein and A. K. Kerman, e-print cond-mat/9804015.
- [7] E. Timmermans, P. Tommasini, R. Côte, M. S. Hussein and A. K. Kerman, e-print cond-mat/9805323.
- [8] Y. Castin, R. Dum, *Phys. Rev. Lett.* **79**, 3553 (1997); P. Nozières in “Bose-Einstein Condensation”, Cambridge (1998), ed. A. Griffin, D. W. Snoke and S. Stringari, 15.
- [9] see e.g. L. van Hemmen, *Fortschritte der Physik* **26**, 397 (1978).

- [10] J. Schwinger, Quantum Theory of Angular Momentum, L. Biedenharn and H. Van Dam Eds., Academic Press, New York 1965.
- [11] J. Schwinger, Quantum Kinematics and Dynamics, W. A. Benjamin, Inc. New York 1970.
- [12] D. Galetti and A. F. R. de Toledo Piza, Physica **A214**, 207 (1995).
- [13] M. C. Cambiaggio, G. G. Dussel and M. Saraceno, Nucl. Phys. **A415**, 70 (1984).

Figure Captions

Figure 1. Energy spectrum of $h^{(AA)}$, Eq. (7), for a symmetric, “weak-laser” case. Units and parameter values are explained in the text. The points below $E \simeq 1$ correspond to nearly degenerate doublets (cf. Fig. 5). Mean numbers of b atoms and the respective variances are shown at the corresponding energy eigenvalues.

Figure 2. Discrete action-angle Weyl transform of the Hamiltonian used in Fig. 1, (a), and the corresponding quasi-classical energy surface, (b).

Figure 3. Discrete action-angle Wigner functions corresponding to the lower (a) and upper (b) member of the lowest doublet in Fig. 1.

Figure 4. Evolution of the probabilities $p(M)$ of the various $|J, M\rangle$ components of the ground-state as a function of the “laser strength” control parameter α . The double-peaked distributions correspond to “Schrödinger cat states”.

Figure 5. Evolution of the integrated level density as a function of J . Other parameters are as in Fig. 1. The quasi-classical limit is also shown.

Figure 6. Typical “small detuning” energy spectrum of $V\mathcal{H}^{(FR)}/J$. Units and parameter values are explained in the text. Mean numbers of molecules and the respective variances are shown at the corresponding energy eigenvalues.

Figure 7. Discrete action-angle Weyl transform of the Hamiltonian used in Fig. 6, (a), and the corresponding quasi-classical energy surface, (b).

Figure 8. Evolution of the integrated level density as a function of J . Other parameters are as in Fig. 6.

Figure 9. Discrete action-angle Wigner function corresponding to the ground state of the spectrum shown in Fig. 6.

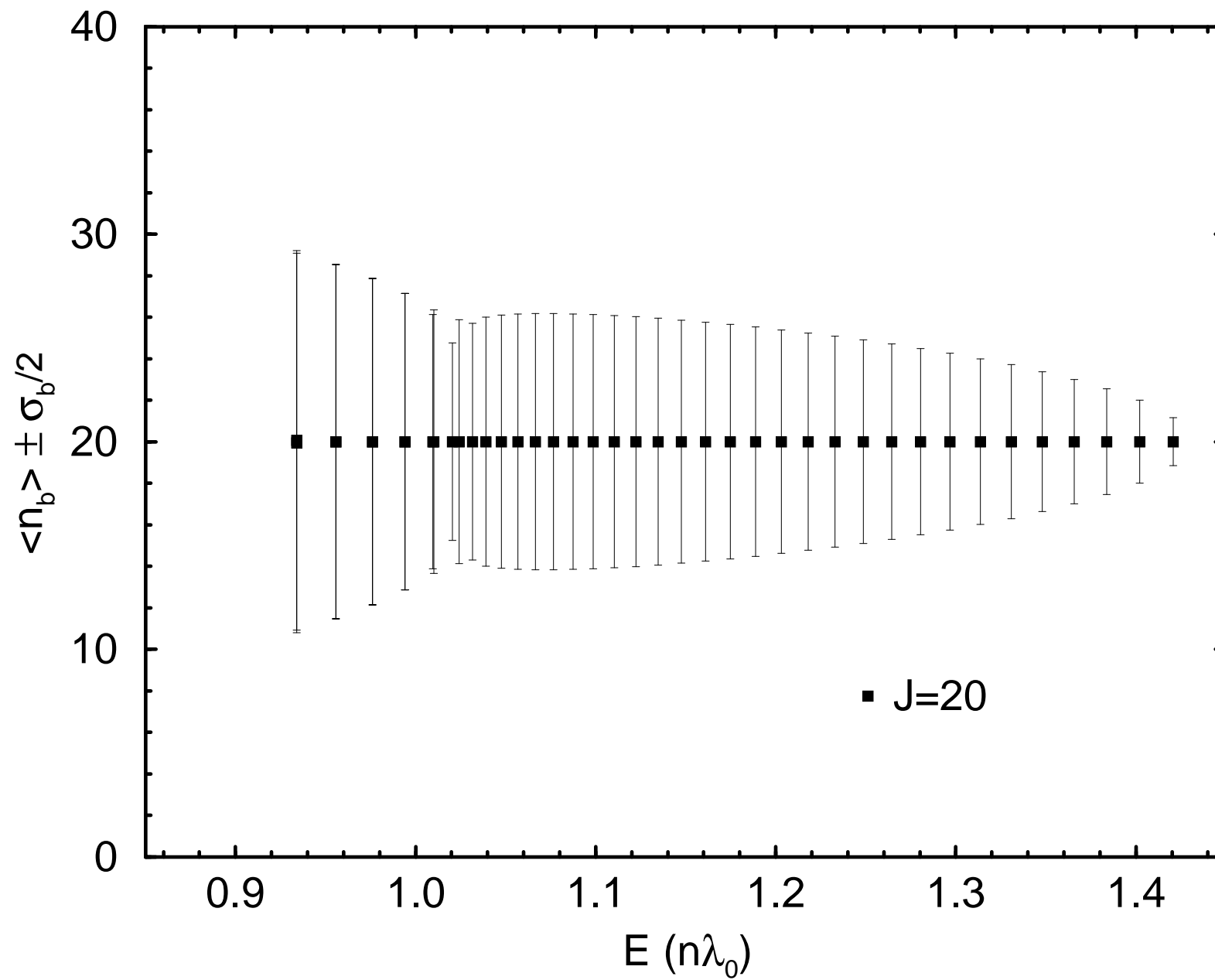
Figure 10. Weyl transform of the Hamiltonian, (a), and Wigner function of the ground state, (b), for “large detuning” $\epsilon_b = 50$. Other parameters as in Fig. 6.

Figure 11. Squared expansion amplitudes of the “large detuning” ground state of Fig. 10 in terms of the “small detuning” eigenstates corresponding to Fig. 6. Results are given for the full $J = 20$ spectrum.

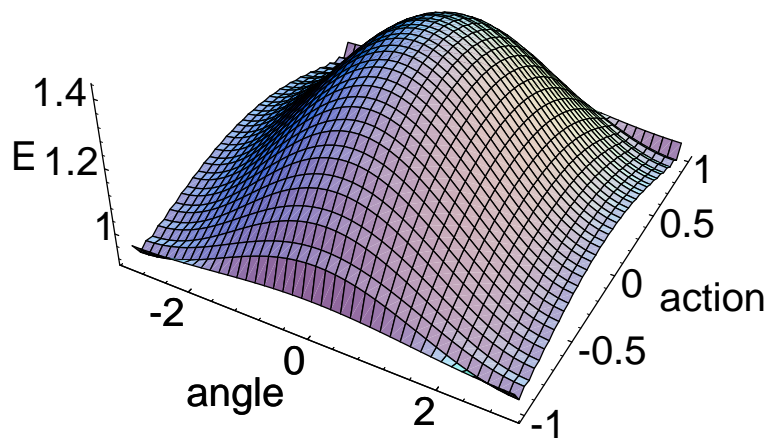
Figure 12. Exact quantum evolution of the “large detuning” ground state under the “small detuning” Hamiltonian for $J = 20$. The heavy curve shows the time evolution of $\langle j_z \rangle$, and the error band shows the time evolution of the root-mean-square dispersion of j_z . Also shown (white squares) is the result of an integration of the quasi-classical Eqs. (16). See text for details.

Figure 13. Numerical solution of the coupled quasi-classical equations (16) and (19). See text for details.

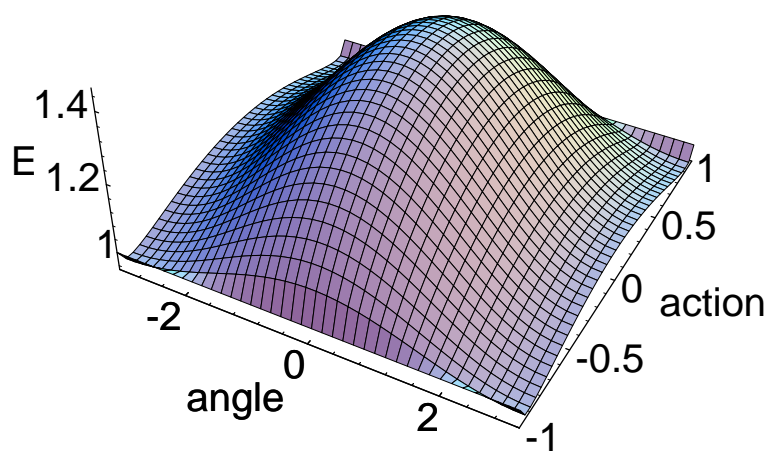
A. N. Salgueiro et al. Fig. 1



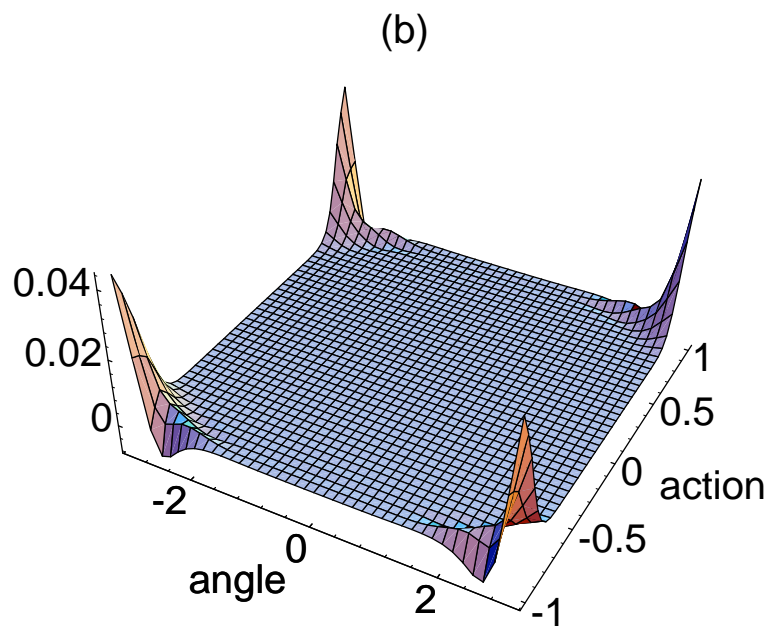
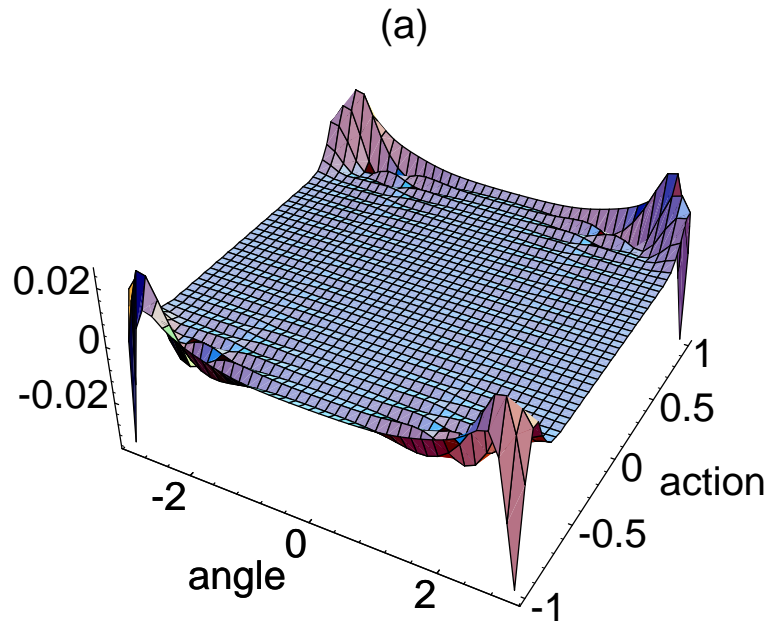
(a)



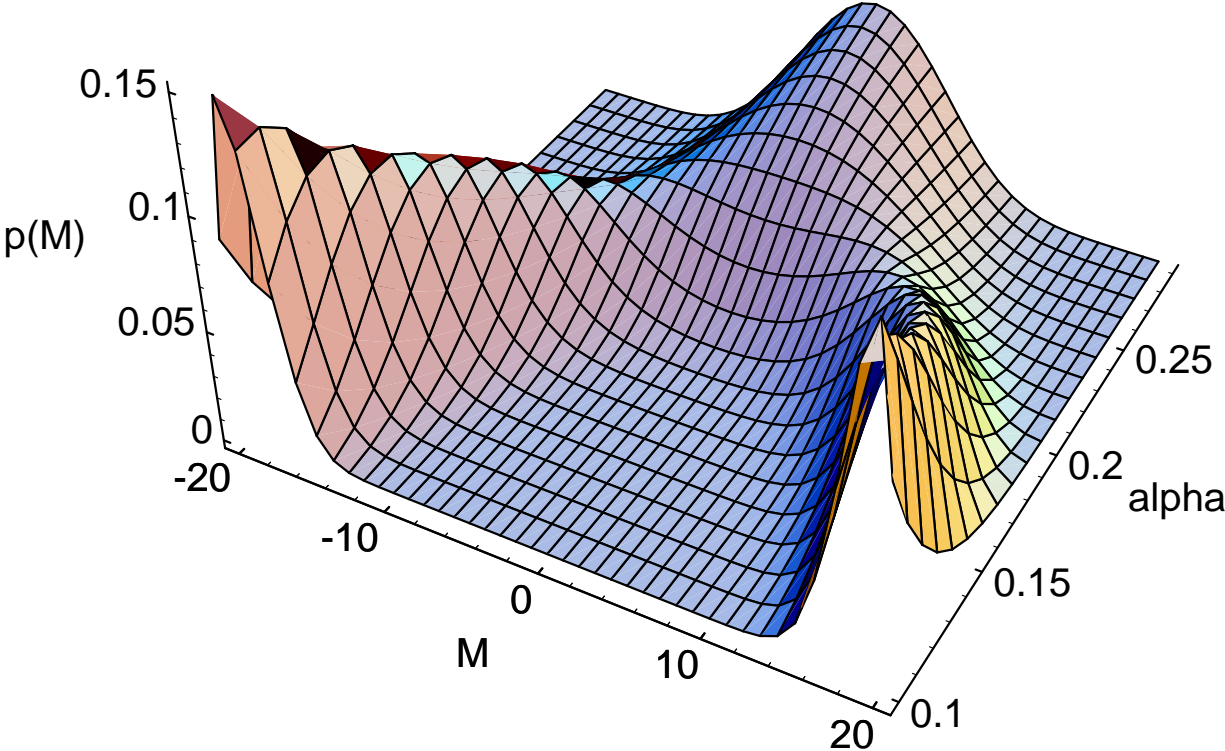
(b)



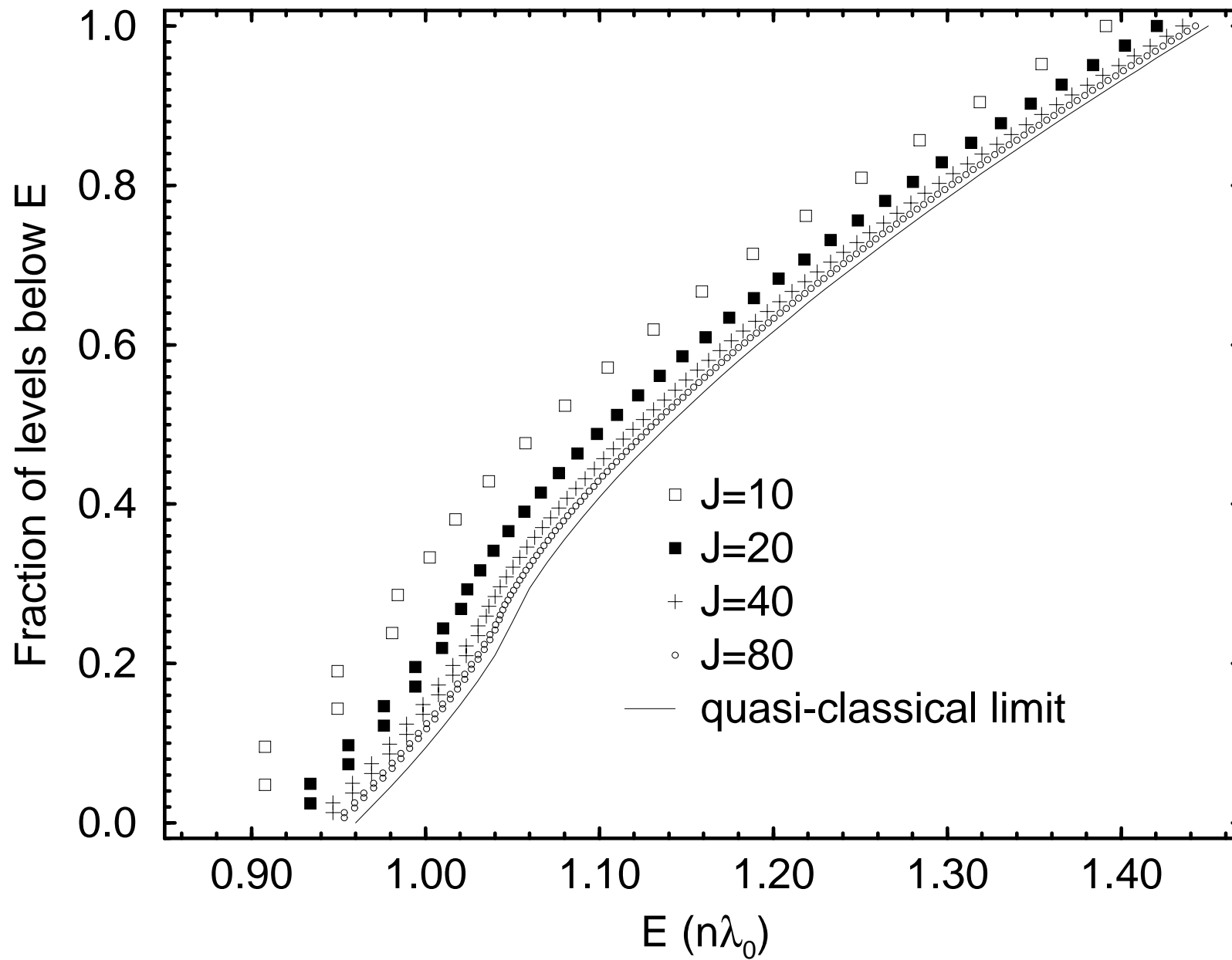
A. N. Salgueiro et al. Fig. 3



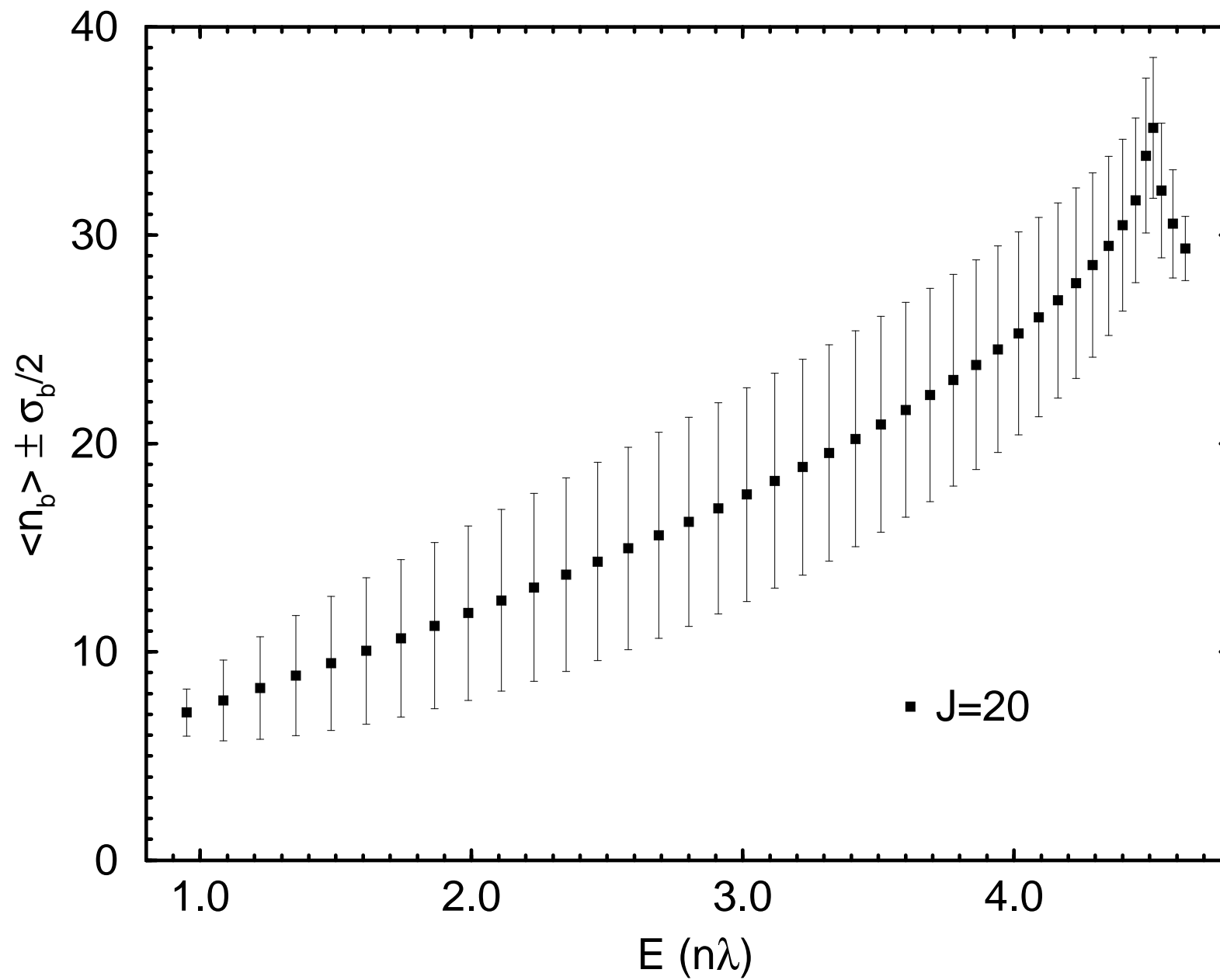
A. N. Salgueiro et al. Fig. 4



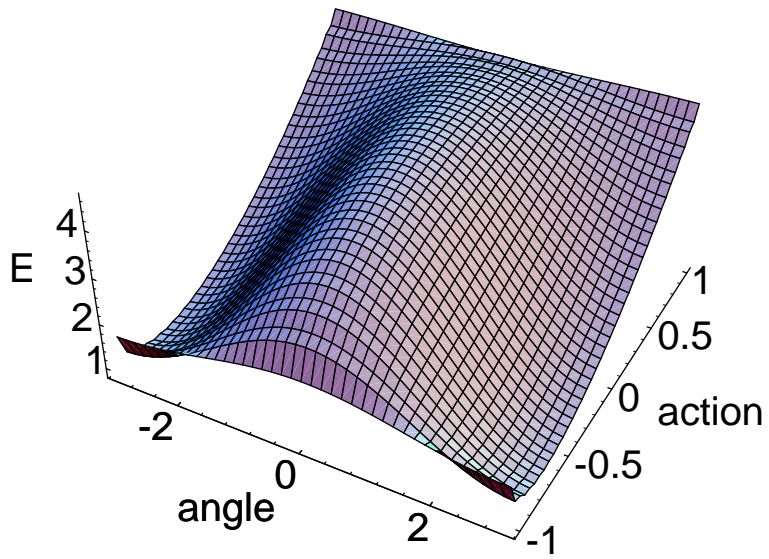
A. N. Salgueiro et al. Fig. 5



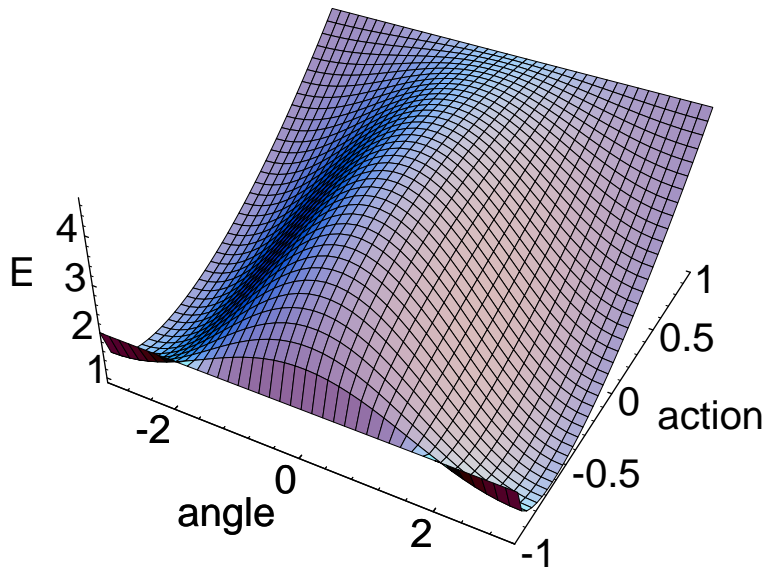
A. N. Salgueiro et al. Fig. 6



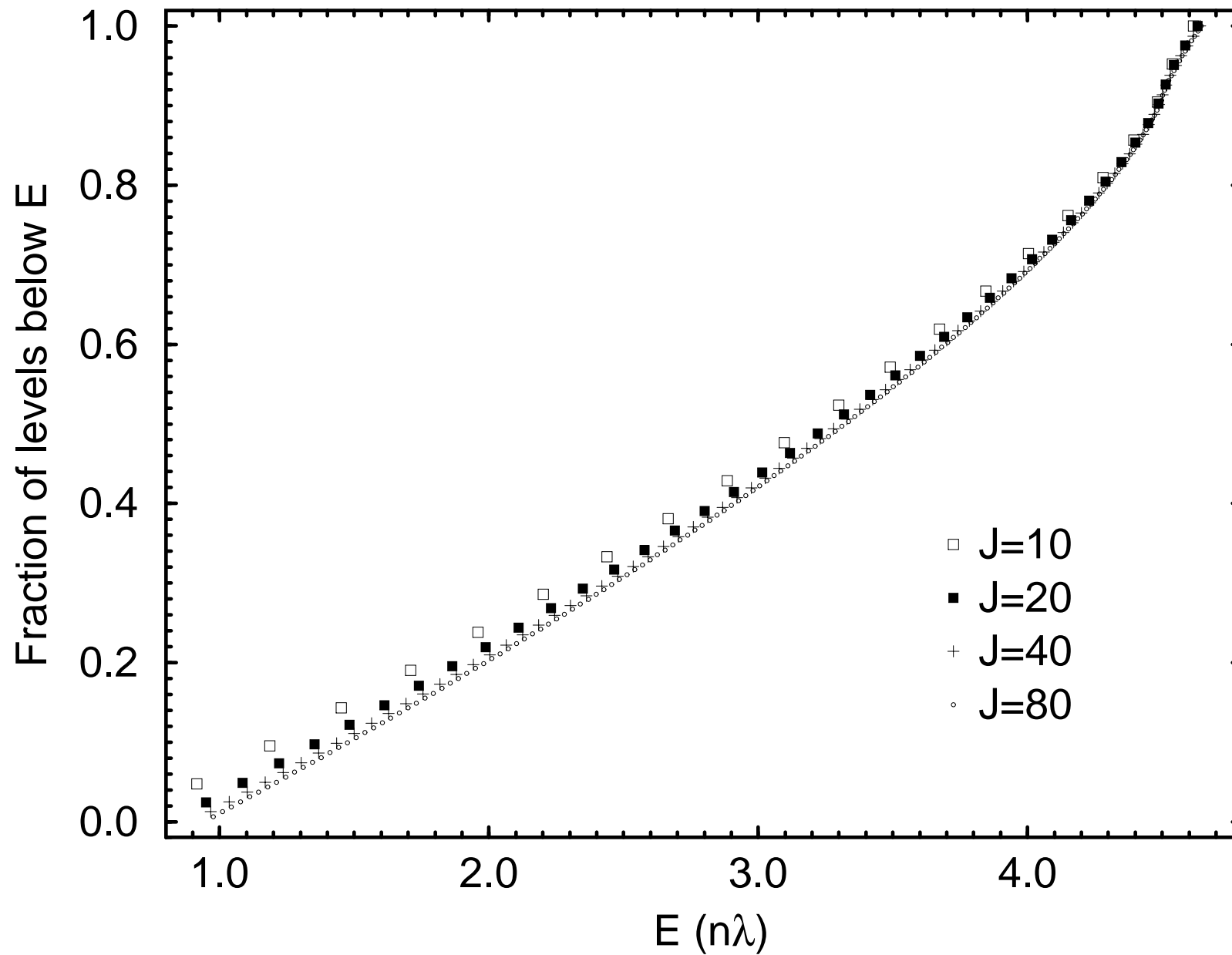
(a)



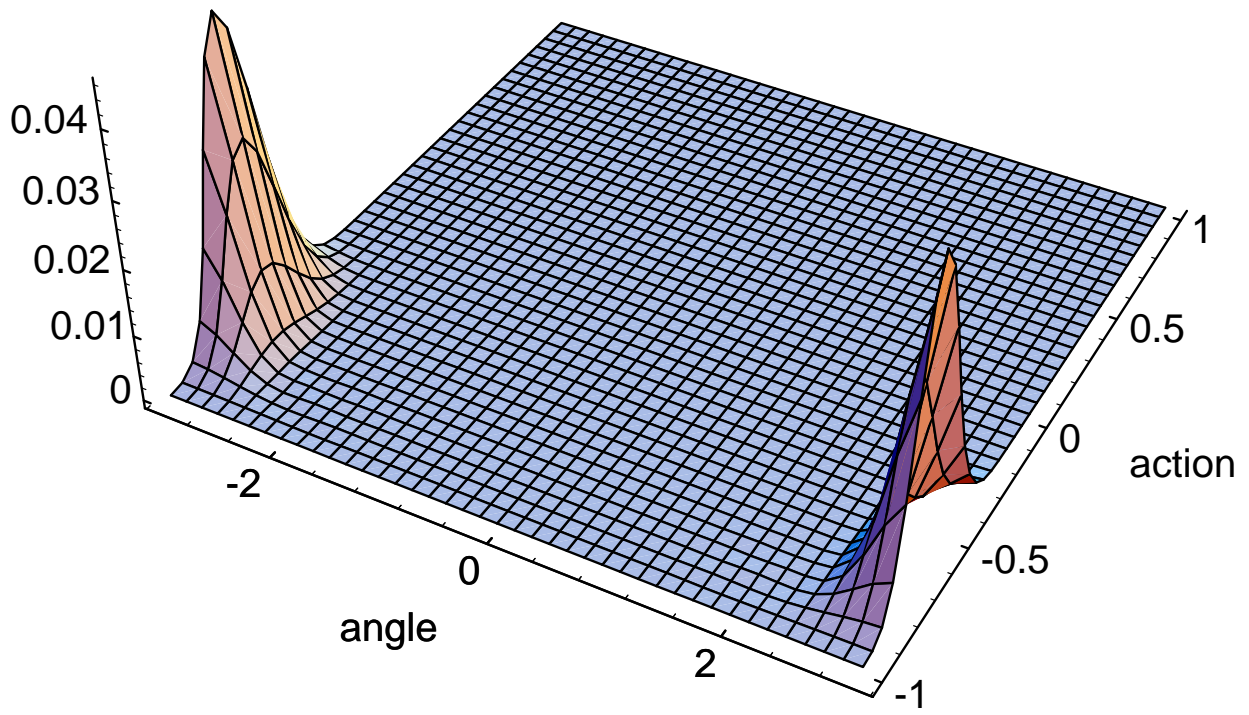
(b)



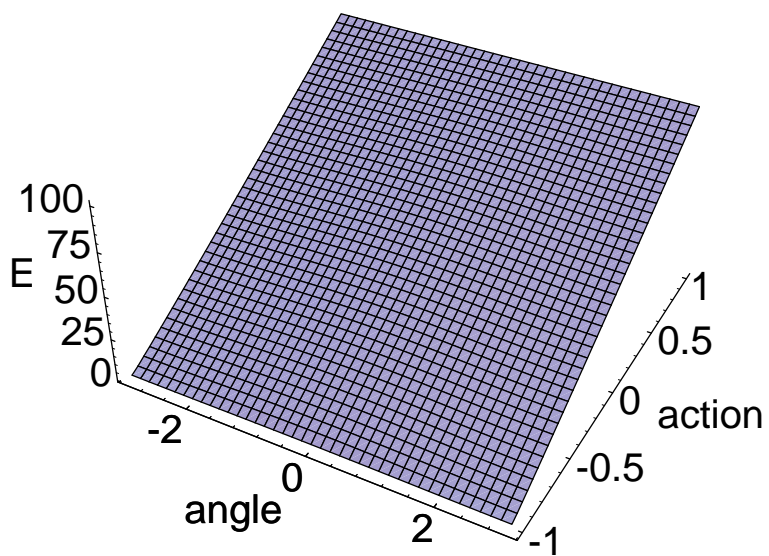
A. N. Salgueiro et al. Fig. 8



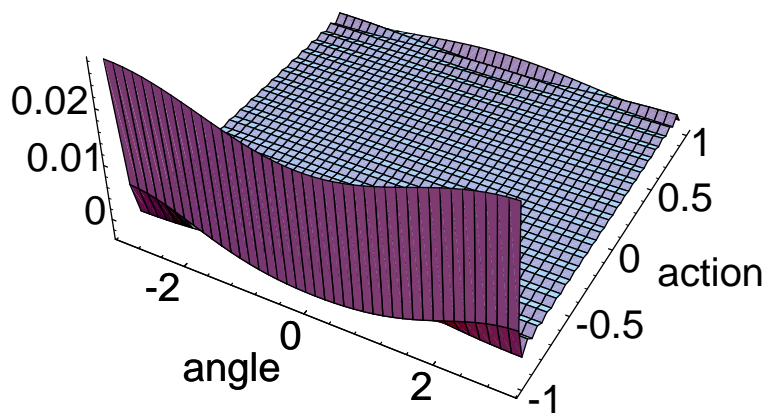
A. N. Salgueiro et al. Fig. 9



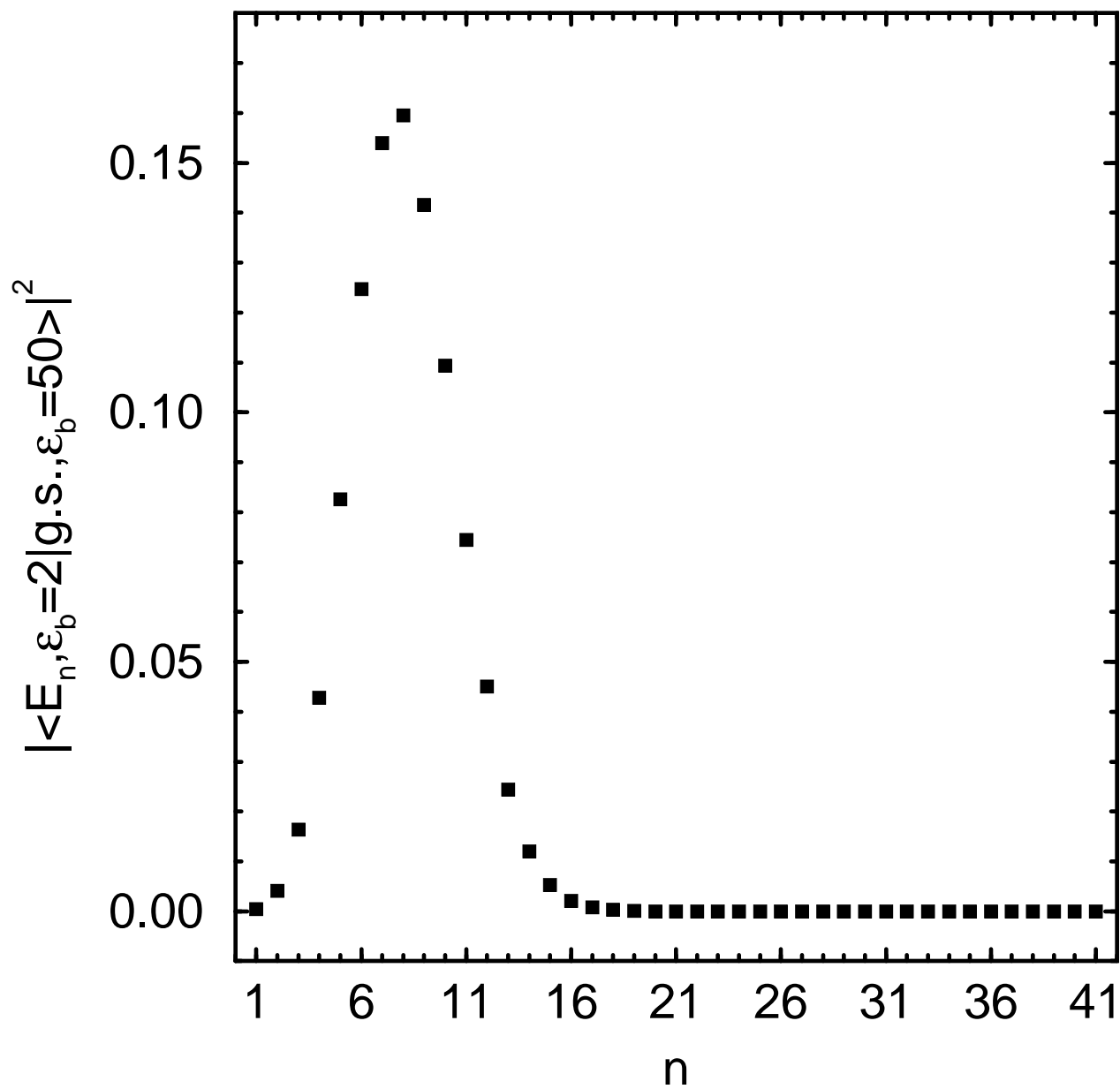
(a)



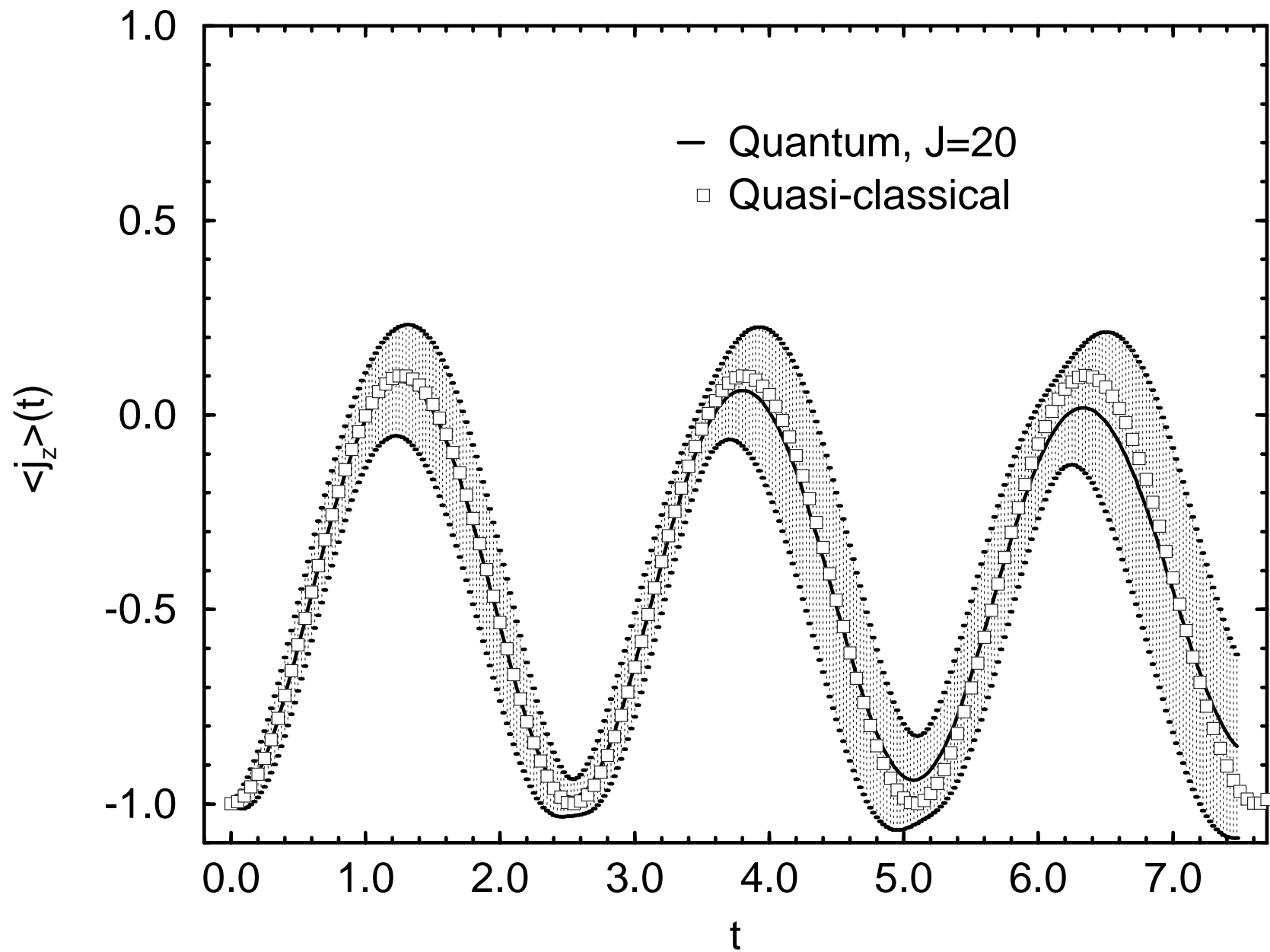
(b)



A. N. Salgueiro et al. Fig. 11



A. N. Salgueiro et al. Fig. 12



A. N. Salgueiro et al. Fig.13

